Journal of Sound and Vibration 329 (2010) 4907–4921

Contents lists available at ScienceDirect

Journal of Sound and Vibration

journal homepage: www.elsevier.com/locate/jsvi

Air-borne sound source characterization by patch impedance coupling approach

Goran Pavić

Laboratoire Vibrations-Acoustique, Institut National des Sciences Appliquées, 20, Avenue Albert Einstein, 69621 Villeurbanne, France

ARTICLE INFO

Article history:
Received 8 October 2009
Received in revised form
1 June 2010
Accepted 2 June 2010
Handling Editor: A.V. Metrikine

ABSTRACT

An approach of independent sound source characterization is discussed. The source is defined by its blocked sound pressure and surface impedance via a suitable enveloping surface. Both the blocked pressure and the impedance are made discrete using the patch averaging concept. The approach is adapted to numerical as well as experimental implementation. The characterization of a source by patches allows for acoustical sub-structuring, which in turn enables the prediction of the sound field created by a source coupled to an arbitrary environment. Numerical simulations are presented which demonstrate the validity of the approach.

1. Introduction

A complex mechanical object often creates noise by the activity of one or several primary noise sources integrated into a passive housing. Typical examples are household appliances such as a dishwasher or a hair-dryer, outdoor machinery such as a lawn-mower or an excavator and power equipment such as a ventilation unit or a refrigeration station. The noise created by the primary source(s) is modified by the housing. The modified noise can be very different to that radiated by the source directly into a free field.

Any reliable noise prediction critically depends on the detailed model of the noise source. Experience shows that the noise of complex sources, like engines, compressors, hydraulic, pneumatic or electrical actuators, etc., cannot be predicted by computation alone. If such a source is taken as a black box its intrinsic noise activity could be found by measurement, using a suitable characterization procedure. The characterization should provide results which are independent of the surrounding space. An independent characterization enables prediction of the coupling of the source to any housing or surrounding, i.e. to any receiver. The requirement on independent characterization is far from being simple. To the best of this author's knowledge, no method has been found so far which is capable of providing an independent and reliable characterization of air-borne sound from a complex source.

A typical noise source not only emits noise in air, but also indirectly, via structure-borne and fluid borne paths. While the characterization methods of structure-borne sources [1–7], and sources in ducts and waveguides [8–14], have been dealt with fairly extensively, the direct air-borne characterization has received less attention, probably because the measurement of air-borne sound is seen as a simple, self-evident task. However, usual noise measurement procedures are not suited for independent and comprehensive characterization of air-borne sources. In particular, the sound power of a source is not a quantity which can be used for an intrinsic source characterization. Not only does the sound power depend on the surrounding, which is often ignored, but it also lacks information on the spatial directivity of the source which can matter a lot where the coupling of the source is concerned.

E-mail address: goran.pavic@insa-lyon.fr

0022-460X/$ - see front matter © 2010 Elsevier Ltd. All rights reserved.
doi:10.1016/j.jsv.2010.06.003

One well-known approach for describing air-borne sound sources substitutes the physical source for a number of simple point sources, such as monopoles [15–19]. Each of these substitute sources may be characterised, frequency by frequency, by a single quantity: its complex volume velocity amplitude. The entire source is then specified with two groups of data: the ensemble of complex amplitudes and the ensemble of spatial positions of the substitute sources. The amplitudes of individual substitute sources are obtained through a classical inversion procedure. Moorhouse and Seiffert [20] have used the substitute source technique to characterise by measurement a small electric motor. The motor was found to be essentially a volume velocity source while the perturbation of the sound field by its small size was negligible. These two conditions have in turn enabled an independent source characterization. However, in most cases the characterization by the substitute source technique will not yield independent results because the acoustics of the receiving space is implicitly included in it.

A comprehensive characterization of an air-borne noise source can be accomplished using a theorem formulated by Bobrovnitskii [21]. It describes the sound field of a system composed of two sub-systems coupled through an enveloping surface. If one of the sub-systems hosts a sound source while the other is passive, the global field can be represented as the sum of two simpler field components. The first component is the field produced by the running source with the enveloping surface fully blocked. This field creates at the enveloping a particular blocked sound pressure. The second component is the field of the coupled sub-systems under the sole action of the blocked pressure acting on the enveloping surface with the source switched off. The principle described enables one to entirely and independently specify the source with two quantities: the blocked pressure and the impedance, both referring to the enveloping surface.

This result has been used to conceive a particular characterization technique for air-borne noise sources [22]. The source is defined in terms of an enveloping spherical surface. The spherical surface represents the enveloping between the source and the receiver space. In this way the physical source is replaced by a substitute one, the purpose of which is to create the same exterior sound field as the original source. The substitute source is the assembly consisting of the physical source and the layer of air between the physical source and the enveloping surface. Due to the spherical shape, the sound field at the interface can be decomposed into spherical harmonics. The number of harmonics is theoretically infinite, but only a limited number of lowest harmonics are taken into account in order to make the decomposition practical. The higher the wavenumber, the larger the number of terms needed for the decomposition.

The substitution of a continuous field by several simple fields, i.e. spherical harmonics, each of which is defined by a single value—its complex amplitude, makes it possible to provide a link between a continuum and a discrete set of values. The same principle is used in the numerical or experimental modal analysis where the theoretically infinite modal summation is replaced by a truncated one. The discrete values are then easily handled by usual matrix formulations which allow one to find the complete source descriptors: the source pressure vector and its impedance matrix.

In order to be used, the spherical harmonics technique requires a particular spherical chamber. This imposes a fairly severe practical constraint. In spite of such a formulation offering a complete and independent result, it requires a specialist's knowledge and a particular experimental test rig which makes it unsuitable for wider use.

The present paper examines an alternative source characterization procedure which could be achieved with less demanding experimental effort than the one described in [22]. The objective is to examine the potential feasibility of the new approach, rather than to solve a particular concrete problem. This is done by considering two cases which can be modelled analytically with sufficient accuracy: a straight tube and a parallelepipedic cavity. Since the new procedure will give an imperfect characterization of the source, it has to be compared with an exact solution in order to establish the characterization error. This explains why the analytical approach has to be chosen at this stage of development.

2. Patch sub-structuring

The principal purpose of independently characterising a source with respect to its noise emission is to predict the noise transmitted to a given receiver space encompassing the running source. The receiver noise will depend on both the source and the receiver. The prediction of the coupling between the two can be then done using sub-structuring. Sub-structuring can be applied in a fairly straightforward way provided the system is linear.

The sub-structuring will normally start by identifying the independent descriptors of the source and of the receiver, i.e. the impedances and the blocked pressure. This is done either by computation or by measurement or both. The coupled state is then found by computation. The latter is done by respecting the acoustical continuity conditions at the sub-system interfaces. The key advantage of sub-structuring from a practical viewpoint is that the identification of a given sub-system can be achieved independently of other sub-systems.

The continuity conditions of mechanical systems are usually expressed in terms of mechanical mobility of the coupled sub-structures. Alternatively the concept of mechanical impedance can be used. Both concepts are well known since a long time ago [23].

The interaction between the sub-systems will rarely be of a local nature. A coupling force in a given point by which one sub-system acts on the adjacent one will affect all of the coupling points. The synthesis can be thus most conveniently done using a matrix formulation of sub-system coupling. The matrix sub-structuring approach is well suited to cases where the sub-systems are coupled via a discrete number of point connections. While a point connection is a theoretical concept which is never strictly valid, it can be applied with a fair degree of accuracy to mechanical systems at lower frequencies where the structural wavelength is significantly larger than the size of the coupling area.

The present approach keeps the concept of an enveloping surface to define the borders of the source sub-system, but returns to the classical definition of impedance [24]. To remove the singularity problem the coupling surface is subdivided into discrete patches, as defined earlier [25]. The quantities involved are then obtained by averaging across the patch surface. In this way each patch can be identified by the averaged value of sound pressure and the normal component of particle velocity. It is clear that averaging by patches makes the present approach necessarily approximate. The smaller the variation of sound pressure and particle velocity across each patch the more accurate the result. This implies that the patches need to be small. Too small patches will be however impractical to deal with and may lead to ill conditioning, especially if the work is based on measurements. Thus one of the key questions is how to define an optimum size of patches under given conditions.

2.1. Governing formulae

To adapt to the impedance concept a sinusoidal time variation with the radian frequency ω is assumed, thus allowing the use of complex amplitudes of the sound pressure $p(t)$, and volume velocity $q(t)$.

Using the patch approach, each acoustical volume Ω concerned is supposed to have a rigid boundary surface S, Fig. 1. An excitation–reception pair of patches of finite size are selected, the first one being the driving patch e, the other one the receiving patch r. In what follows, the patch impedance Z_{re} will be defined as the ratio of the complex amplitude sound pressure, P_r, averaged across the receiving patch ΔS, and the complex amplitude of the volume velocity excitation, Q_e, averaged across the excitation patch ΔS_e:

$$Z_{re} = \frac{\langle P_r \rangle_{\Delta S}}{\langle Q_e \rangle_{\Delta S_e}}, \quad p_r(t) = P_r e^{j\omega t}, \quad q_e(t) = Q_e e^{j\omega t} \tag{1}$$

where the triangular brackets denote spatial average. The unit of the patch impedance defined by Eq. (1) is $\mathrm{Ns/m^5}$. The patch volume velocity is the integral of the normal component of particle velocity v_e across the patch surface:

$$q_e = \int_{\Delta S_e} v_e \, dS, \quad \Delta S_e \in S \tag{2}$$

The source has to be characterised by its blocked pressure p_b and its impedance $Z_{s,cc}$, both relative to the coupling surface selected for source characterization [22]. If the number of patches is N, the blocked pressure will be an $N \times 1$ vector $\mathbf{p}_b$ and the source coupling impedance an $N \times N$ matrix $\mathbf{Z}_{s,cc}$. The surrounding reception space will be characterised using the same coupling surface by an $N \times N$ reception–space interface impedance matrix $\mathbf{Z}_{r,cc}$. In such a case the vectors expressing coupling volume velocity amplitudes and coupling pressure amplitudes, $\mathbf{Q}_c$ and $\mathbf{P}_c$, read [22]:

$$\mathbf{Q}_c = (\mathbf{Z}_{s,cc} + \mathbf{Z}_{r,cc})^{-1} \mathbf{P}_b, \quad \mathbf{P}_c = \mathbf{Z}_{r,cc} \mathbf{Q}_c \tag{3}$$

Once the coupling pressure has been found, the sound pressure amplitude vector $\mathbf{P}_a$ at K points in the reception space can be found using a $K \times N$ reception impedance matrix $\mathbf{Z}_{r,ac}$:

$$\mathbf{P}_a = \mathbf{Z}_{r,ac} \mathbf{Q}_c \tag{4}$$

Eqs. (1) and (2) are formulated in the frequency domain, meaning that the application of these equations has to be made frequency by frequency.

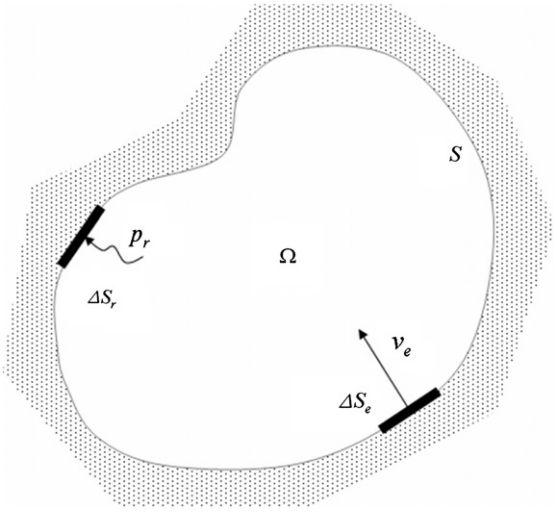

Fig. 1. Definition of patch impedance (note that the interface surface has to be blocked).

2.2. Demonstration of source–receiver coupling using patch approach

In order to illustrate in a simple way the acoustical coupling source–receiver by the patch method a textbook example is provided in this section. The entire acoustical system consists of a straight tube driven by a flat piston at one end and closed by a uniform impedance Z_e at the other end, Fig. 2. In such a case only plane waves exist which greatly simplifies the analysis.

This simple case is presented in Appendix A. It is shown that a direct computation of sound pressure in an arbitrary point gives strictly the same result as the computation done by patch sub-structuring. However, even in this simple case the sub-structuring technique will produce errors if the descriptors of the system, the source pressure and the two impedances, are perturbed by noise. Such noise contamination can occur in measurements. In order to illustrate ill effects of perturbation by noise, the following numerical values will be used: tube length l=0.9 m, tube diameter d=10 cm, sound speed c=343 m/s, mean mass density ρ_0=1.21 kg/m^3, air kinematic viscosity $\mu=1.51\times10^{-5}$ Ns/m^2, and coordinate of the interface plane a=0.4 m. The non-driven end of the tube is taken to be a baffled opening. Its impedance is approximated by that of a circular piston inserted in a baffle ([26], Chapter XI):

$$Z_s=\frac{\rho_0 c}{\mathrm{j}S}\left[1-2\frac{J_1(kd)}{kd}+2\mathrm{j}\frac{S_1(kd)}{kd}\right] \tag{5}$$

where J_1 and S_1 stand for first-order Bessel and Struve functions. The dissipation in air due to viscosity is accounted for by a complex wavenumber, the imaginary part of which equals $k_i=(2/3)\mu k^2/\rho_0 c$ ([27], Chapter XIX).

Fig. 3 shows the modulus of the coupling pressure amplitude P_c. To emphasize the ill effects of imperfect input data, the coupling pressure is presented by two values: the exact one and the one obtained by injecting random noise of 50 dB signal-to-noise ratio (S/N). The noise was injected by adding sequences of random complex values to the original functions. A simple sequence was added to the blocked pressure file. Its global RMS value was 50 dB lower than that of the pressure. In the case of two impedances, adding the noise was done by splitting each impedance function into two functions, one for

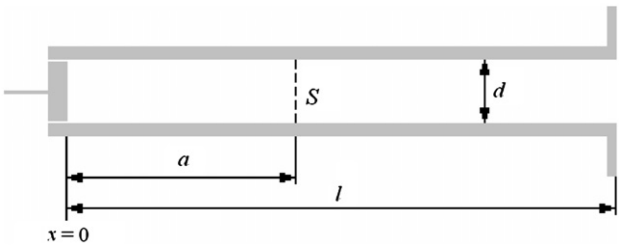

Fig. 2. Simple tube demonstrator.

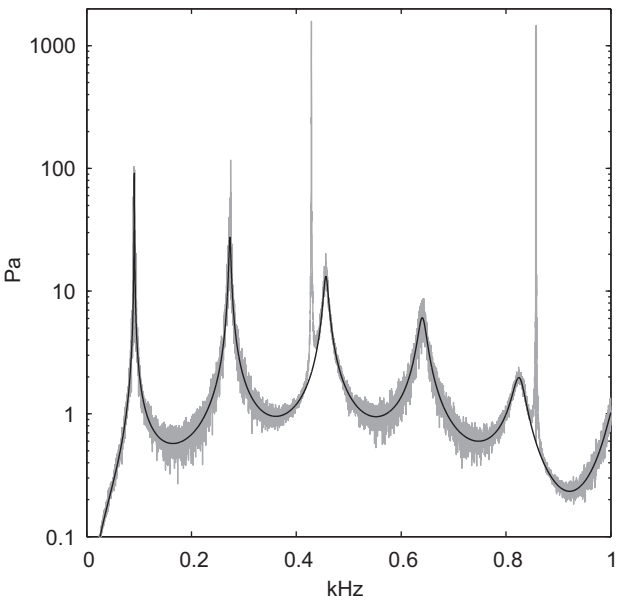

Fig. 3. Tube demonstrator: normalised coupling pressure at the interface source–receiver. ————: exact value; ————: values contaminated by noise.

the response, the other for the excitation, and by adding random noise to each of these before taking the ratio of the two. In this way realistic measurement conditions could be simulated.

It can be seen that the noise contamination of the computed coupling pressure is very high in spite of the fairly low noise level of the input quantities to sub-structuring, i.e. Z_s, p_b, and Z_r from which the coupling pressure has been obtained. Moreover, at frequencies equal to resonance frequencies of the blocked source the computed coupling pressure exceeds the true value by several orders of magnitude.

An important conclusion can be drawn from the present simple example: if the input quantities to sub-structuring are contaminated by noise, the resulting output is likely to be much noisier than the input data and the error in the result may increase considerably at some discrete frequencies.

2.3. 3D patch coupling of parallelepipedic spaces

The coupling by patches will produce two types of errors: a discretisation error inherent to the patch coupling method and a measurement error in cases where the source and receiver descriptors are identified by measurement. The first type of error will appear in all but the most simple cases, such as the one discussed in §2.2. The second type of error will be due to imperfect input data when these are provided by measurement.

In Appendix B formulae are derived for patch sub-structuring applied to parallelepipedic spaces. Both the source and the receiver are modelled as parallelepipedic acoustical volumes. Such a geometry enables the use of an analytical solution which is needed in the analysis to follow.

It has been shown in Appendix B that the spatial average of either the response sound pressure or the excitation volume velocity across a given patch of surface ΔS can be obtained by ordinary modal superposition of the form given by Eq. (B1) by multiplying the mode functions ϕ_n by patch weighting factors $\gamma_{x,n}$, $\gamma_{y,n}$ or $\gamma_{z,n}$ defined in Eqs. (B6) and (B7). Eq. (B1) gives the sound pressure in a point due to point source excitation, while the patch averaging can result in one of the following cases which will be considered in the next section:

(1) excitation by a point volume source of strength Q at $\mathbf{r}_e$, pressure response averaged across a patch ΔS centred at $\mathbf{r}$:

$$\langle P(\mathbf{r})\rangle_{\Delta S} = Q(\mathbf{r}_e)\sum_n \boldsymbol{\Phi}_n(\mathbf{r},\mathbf{r}_e,\omega)\gamma_n(\mathbf{r}) \tag{6}$$

(2) excitation by a volume source of total strength Q averaged across a patch ΔS_e centred at $\mathbf{r}_e$, pressure response at a point $\mathbf{r}$:

$$P(\mathbf{r}) = \langle Q(\mathbf{r}_e)\rangle_{\Delta S_e}\sum_n \boldsymbol{\Phi}_n(\mathbf{r},\mathbf{r}_e,\omega)\gamma_n(\mathbf{r}_e) \tag{7}$$

(3) excitation by a volume source of total strength Q averaged across a patch ΔS_e centred at $\mathbf{r}_e$, pressure response averaged across a patch ΔS centred at $\mathbf{r}$:

$$\langle P(\mathbf{r})\rangle_{\Delta S} = \langle Q(\mathbf{r}_e)\rangle_{\Delta S_e}\sum_n \boldsymbol{\Phi}_n(\mathbf{r},\mathbf{r}_e,\omega)\gamma_n(\mathbf{r})\gamma_n(\mathbf{r}_e) \tag{8}$$

Eq. (6) will be used to get the blocked sound pressure at any interface patch ΔS due to one or several point sources located within the source cavity. Eq. (7) will be used to get a point response in the receiver cavity, excited by interface patch velocity ΔS_e, as formulated in Eq. (4). The last equation will be used to get a patch-averaged response due to patch excitation. In particular, it will be used to produce a patch-to-patch impedance Z_{re} as defined by (1):

$$Z_{re} = \sum_n \boldsymbol{\Phi}_n(\mathbf{r},\mathbf{r}_e,\omega)\gamma_n(\mathbf{r})\gamma_n(\mathbf{r}_e) \tag{9}$$

3. Approach validation

This next study will be a 3D generalisation of the simple tube example. Its objective is to introduce the matrix formulations defined by Eqs. (3) and (4) and to check the validity of the descriptors based on patch coupling. Both the source and the receiver will be modelled as parallelepipedic acoustical volumes using Eqs. (7)–(9). The two will be coupled in such a way that the entire system is again a parallelepipedic space. The latter is needed to provide a direct analytical solution to the sound pressure at the reception point in parallel to the solution obtained by the patch approach. The comparison of two solutions will be used to serve as a validation of the patch approach.

3.1. The system

The walls are lightly absorbing, having an absorption coefficient α. The entire volume is divided by a fictitious surface into two cavities, the source cavity Ω_s and the receiver cavity Ω_r, Fig. 4.

The overall system length and the position of the source–receiver interface will be kept the same as in the tube example, i.e. 0.9 and 0.4 m. While in the tube case the lateral size was of no importance owing to the plane-wave character

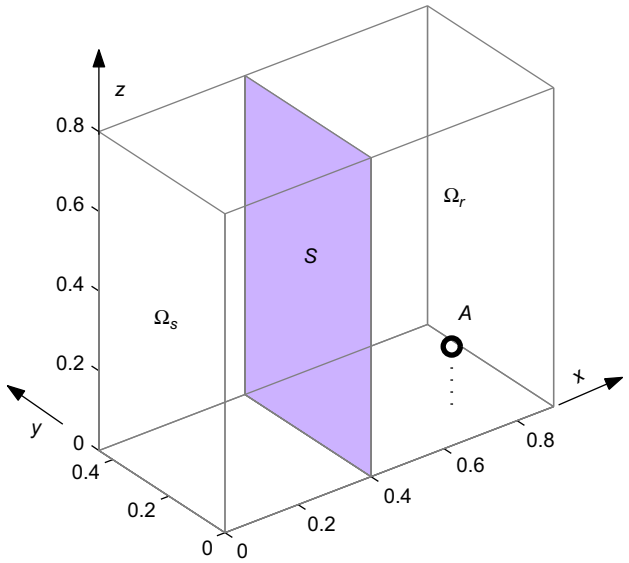

Fig. 4. 3-D source and receiver configuration.

of sound field, in the present case the width and the height of the cavity do matter: these will be taken 0.45 and 0.8 m, respectively. The receiving point position was chosen at random as [0.7292, 0.1409, 0.1464] m.

The frequency range was selected to coincide with the 500 Hz octave band, i.e. spanning from 354 to 707 Hz. The frequency, being linked to the wavelength, affects the patch spatial averaging and thus its optimum size. One octave band was considered to be a good compromise between the need to have wide enough frequency coverage and yet narrow enough width which can be easily associated to a representative single frequency: the band centre frequency. Had the band been larger, the notion of centre band frequency would not have been clear. To this end any octave band could have been chosen, however the 500 Hz band was believed to be well representative of typical noise problems.

It is known that very large number of modes need to be taken into account where patch coupling is concerned. In order to meet this requirement a residual mode solution can be applied for patch modelling [29]. The residual mode approach is needed in various applications where the result depends critically on detailed modal superposition, e.g. in the computation of intensity [30]. In the present paper the solution is found analytically, thus a very large number of modes could be used instead of resorting to the residual mode solution. In this way the convergence of the solution with the increase of number of modes could be monitored. In the current case all the modes having the natural frequencies up to 20 kHz, were included in the computation. This corresponds to some 277,000 modes for the entire system. Such a large number is not needed in direct computation of sound pressure, but is needed with the patch coupling approach.

The coupling surface was subdivided into 24 patches, Fig. 5. The patch average size was about 11 cm $\times$ 13 cm, i.e. about 20% of sound wavelength at the middle frequency of the band analysed.

The patches were made unequal, using a 20% random variation of sizes around mean values. As a matter of fact there is no need for the patches to be of equal shape, so the present choice was used as an additional test of the method.

In the case studied the first 30 modes cover the 0–1 kHz band in terms of natural frequencies and thus provide principal contribution to the generation of sound pressure within the selected 500 Hz octave band. If one analyses how the modal integers, equal to the number of modal half-wavelengths at the coupling surface, change for the first 30 modes one finds that in both y and z directions the criterion of minimum two patches per modal wavelength is amply satisfied.

3.2. Excitation by two pistons embedded in the wall

In analogy with the tube case, the excitation will be provided by a piston motion of the wall at $x=0$. If the wall was to move uniformly, the tube conditions would have been repeated. In such a case the sound would have consisted of plane waves only, meaning that only the modes in the x-direction would have been excited. In order to set all the modes into motion, the excitation is provided at the face $x=0$ by two oscillating pistons. The y- and z-positions of pistons' centres were chosen at random, the same as the amplitudes and phases. The complete set of piston parameters is given in Table 1:

The volume velocity complex amplitudes of the two pistons were kept the same at all frequencies: $Q_1=1\times10^{-3}$and $Q_2=2\mathrm{j}\times10^{-3}$ m^3/s.

The independent source descriptors, its blocked pressure p_b and its impedance $Z_{s,cc}$ at the coupling surface S, were then computed using Eqs. (6) and (9), respectively. Figs. 6 and 7 show the RMS values of the blocked and coupling pressures, p_b

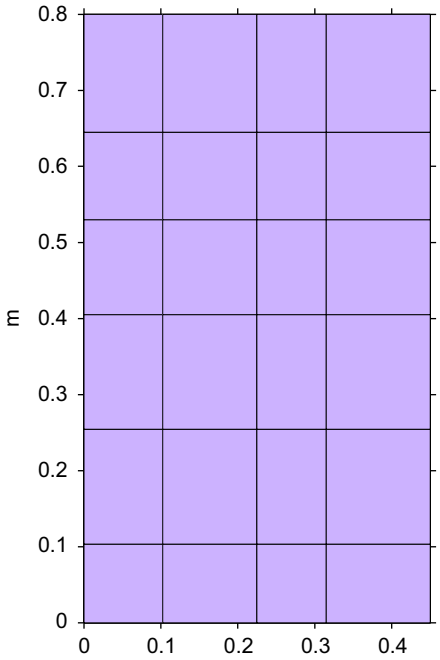

Fig. 5. Coupling patches.

Table 1
Parameters of excitation by two pistons.

Piston	*y* pos. (m)	*z* pos. (m)	Width (m)	Height (m)
1	0.2682	0.6176	0.15	0.25
2	0.1616	0.1184	0.25	0.15

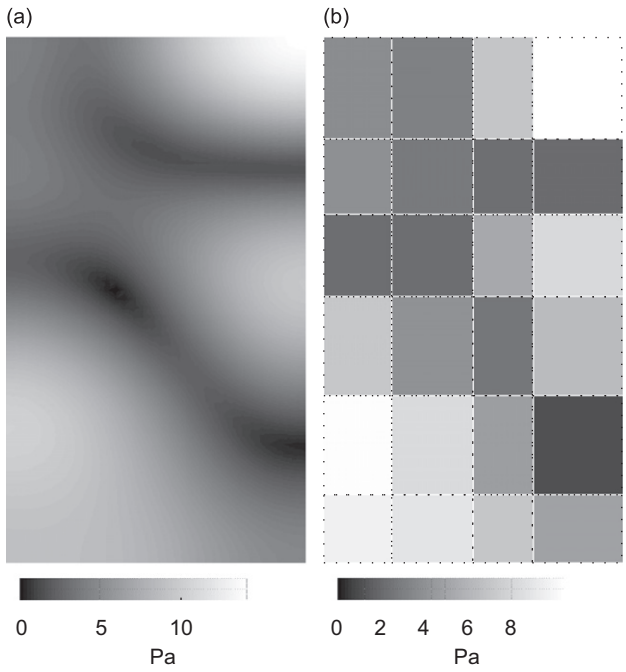

Fig. 6. Continuous (a) and patch-averaged (b) RMS blocked sound pressure across the interface surface at 670 Hz.

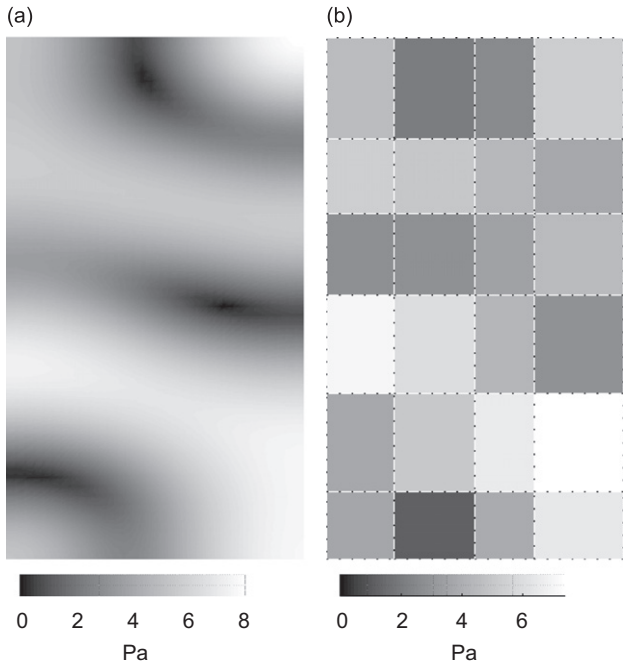

Fig. 7. Continuous (a) and patch-averaged (b) RMS coupled sound pressure across the interface surface at 670 Hz.

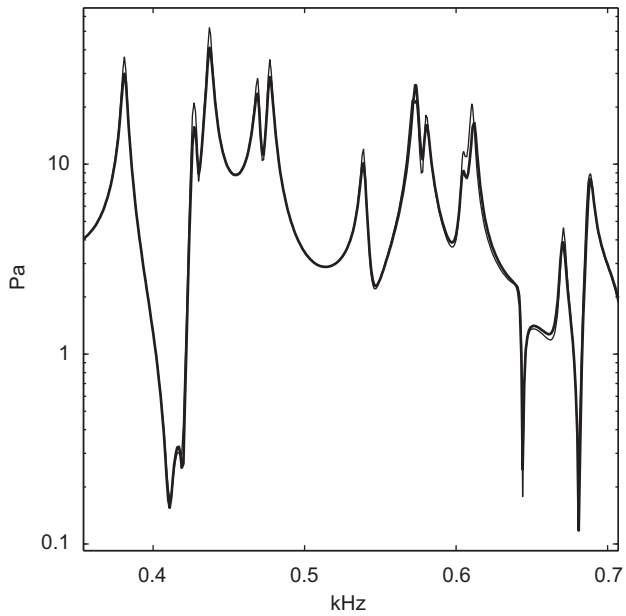

Fig. 8. Excitation by two pistons: RMS sound pressure at the reception point. ——: solution by patch coupling; —: exact solution.

and p_c, at a single frequency chosen at random, f=670 Hz. Each pressure is presented in two formats: exact and averaged by patches. Quite naturally, the coupled pressure pattern is more complex due to involvement of larger number of modes (larger cavity) which effectively contribute to pressure formation. The averaging of pressure across patches gives an impression of causing loss of fine detail contained in the true pressure distribution.

The validation of the patch coupling method was done by comparing the sound pressure at the reception point A computed by the patch method with the exact values. The latter were obtained using Eq. (7), by considering the entire cavity as a single space. The pressure at the reception point using the separate source and receiver models was then computed using sub-structuring through Eqs. (3) and (4).

The RMS sound pressure at the reception point is shown in Fig. 8. The result obtained by patch coupling is seen to stand very close to the directly obtained solution. The matching was found to be very good both in amplitude and in phase. The peaks of the RMS pressure are slightly chopped off with respect to the exact values as a result of patch spatial averaging.

The frequency range analysed, i.e. 354–707 Hz band, contains three 1/3 octaves, centred at 400, 500, and 630 Hz. The difference between the patch-averaged and exact values expressed in 1/3-octave RMS values are −2.62, −1.71, and −0.52 dB, respectively.

3.3. Uneven excitation across the entire wall

In order to further check the validity of the approach, an alternative excitation was selected by 8 oscillating pistons, covering the entire wall at $x=0$. The surfaces and centre point positions of the pistons were selected at random, dispersed within ±40% of the mean values. The amplitudes and phases of volume velocities of different pistons were also chosen at random. The initially chosen values of complex velocity amplitudes were then corrected to provide zero mean volume velocity, Table 2. The whole excitation array was in fact conceived to create poor radiation conditions: short surface wavelengths combined with zero volume velocity. This spatial excitation was then applied to all frequencies. The patch geometry of the coupling interface was kept the same as in the previous example.

Fig. 9 compares the RMS sound pressure at the reception point obtained once by patch coupling and then by the exact solution. In spite of the fairly complex excitation pattern employed, the two results stay remarkably close to each other. The difference between the patch-averaged and exact values expressed in 1/3-octave RMS values are −1.53, −1.82, and −1.78 dB, respectively.

Table 2
Parameters of excitation by eight pistons.

Piston	y pos. (m)	z pos. (m)	Width (m)	Height (m)	Vol. strength (cm^3/s)
1	0.1688	0.1410	0.3375	0.2819	−3.9035+3.4798i
2	0.3938	0.1410	0.1125	0.2819	−1.3230−2.5540i
3	0.1688	0.3289	0.3375	0.0940	−0.0455+7.1804i
4	0.3938	0.3289	0.1125	0.0940	−0.1263−2.1360i
5	0.1688	0.4560	0.3375	0.1603	7.9751−3.0829i
6	0.3938	0.4560	0.1125	0.1603	1.3430+5.4685i
7	0.1688	0.6681	0.3375	0.2638	−0.1245−0.9529i
8	0.3938	0.6681	0.1125	0.2638	−3.7953−7.4030i

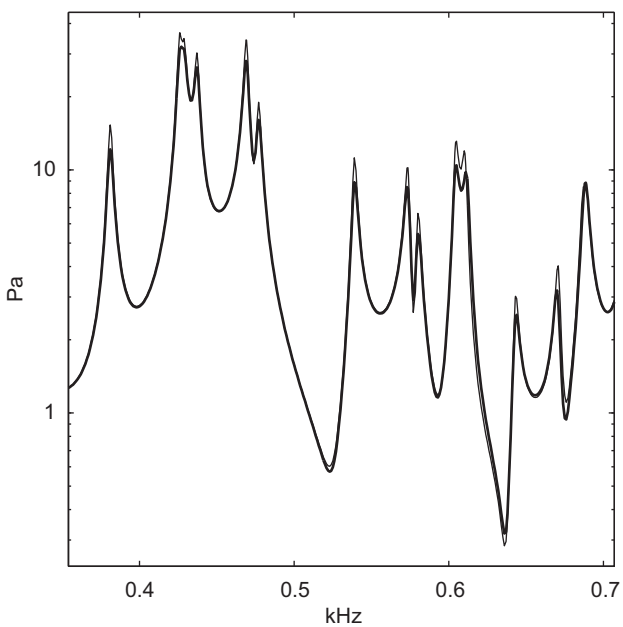

Fig. 9. Excitation by eight oscillating pistons embedded in the wall: RMS sound pressure at the reception point. ——: solution by patch coupling; —: exact solution.

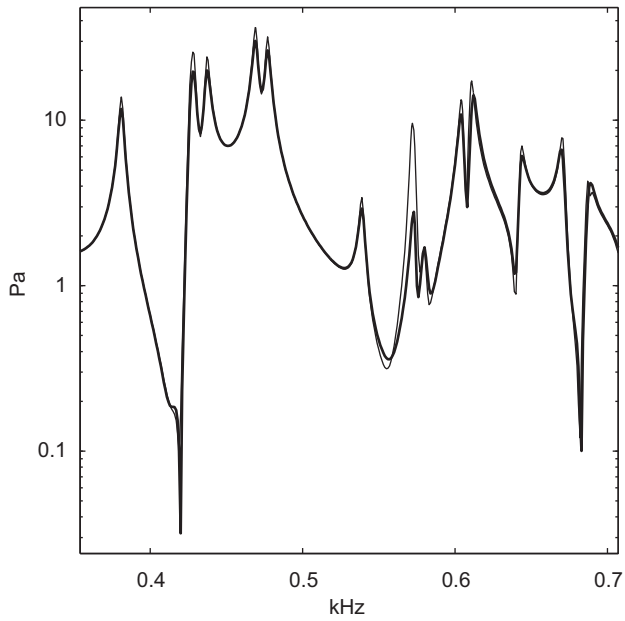

Fig. 10. Excitation by interior point sources: RMS sound pressure at the reception point. ——: solution by patch coupling; —: exact solution.

3.4. Excitation by interior point sources

A final validation was done using point sources as primary excitation, placed within the source part of the cavity. Two monopoles of complex amplitudes $Q_1 = 1 \times 10^{-3}$ and $Q_2 = 2\mathrm{j} \times 10^{-3}$ m^3/s were placed at two points chosen at random: [0.1176, 0.2682, 0.3860] and [0.2352, 0.1616, 0.0740] m, respectively. The same coupling patch pattern was used as in the two previous examples.

A comparison of RMS pressures obtained by patch coupling and by the direct solution is given in Fig. 10. Again a good matching was obtained, however this time with local mismatch around 570 Hz somewhat stronger than in the preceding examples. The stronger mismatch is attributed to the point excitation which produces a pressure pattern more sensitive to details than an excitation spread over a portion of a surface. The difference between the patch-averaged and exact values expressed in 1/3-octave RMS values is again negative -2.79, -1.72, and -2.81 dB, respectively.

The results obtained so far are considered to have validated the patch approach of characterising the source by its blocked pressure and impedance.

3.5. Measurement perspectives

As pointed out earlier, an important field of application of the patch coupling approach could be the characterization of a sound source by measurement. The source and receiver descriptors, p_b, z_s, and z_r, can be obtained in principle by multiple point measurements, using a small loudspeaker as a "point" source. Alternatively a surface transducer could be used for either patch excitation or patch response. With the present-day technology however patch sensors do not provide enough electro-acoustical sensitivity for source characterization work.

If point transducers are used the main issue is how to achieve patch averaging. This can be in principle done by simultaneous multi-point pickup/actuation within the patch area followed by averaging of the acquired signals. Another solution would be to apply a suitable wiring of the transducers of the patch array to create a single output signal or a single actuation signal. Fig. 11 depicts the principle of measuring the blocked source pressure and the receiver impedance.

Perhaps the biggest difficulty in applying the impedance patch approach is to make sure the boundaries of the interface surface are rigid. This condition, required by the definition of impedance, can be achieved in practice if the surfaces are made very stiff and free from own resonances. It is unlikely that such severe constraints can be fulfilled for large surfaces. A way to circumvent this difficulty would be to carry out measurements using non-rigid interfaces and to re-compute the results for the case of rigid surfaces. In this case unfortunately the patch impedance of the actual surface has to be known, i.e. has to be measured, which increases the volume of experimental work.

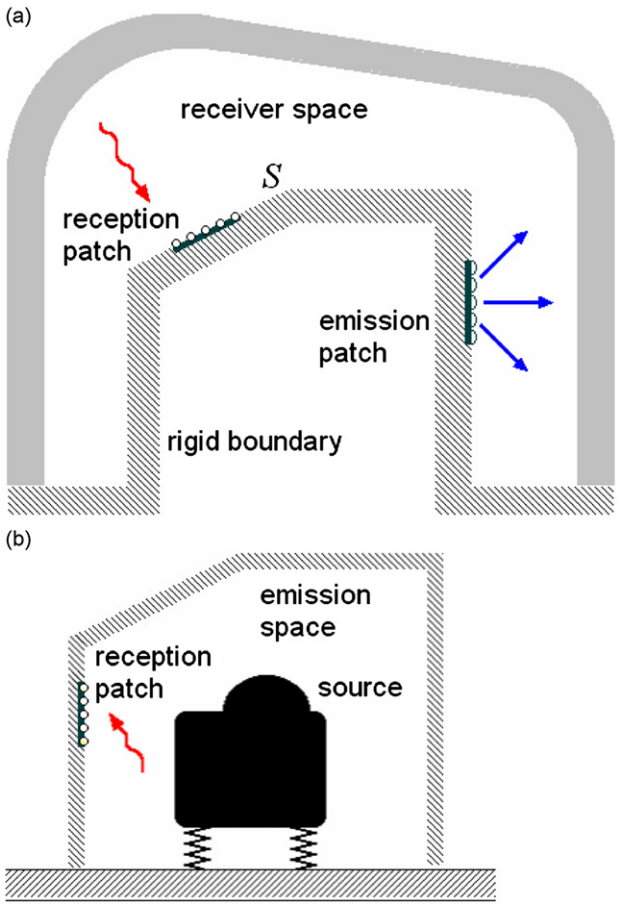

Fig. 11. Measurement of patch-averaged quantities: (a) source blocked pressure and (b) receiver impedance.

Insufficient rigidity of interface surfaces is not the only difficulty one can expect in measurements. As a rule, inevitable measurement errors may severely damage the performance of the patch approach. Fig. 12 shows the sound pressure obtained in the case of two-piston excitation where the three inputs, p_b, Z_s, and Z_r, were all contaminated by random noise of 50 dB S/N ratio in the way explained in the Section 2.2. The results were obtained over a population of 100 different realisations of signal contamination. The grey zone represents the area between maximum and minimum values. One can see that the discrepancy between the erroneous and exact results, taken frequency by frequency, is at some frequencies quite significant, of an order of magnitude or even more. The largest spread of results systematically occurs in the vicinity of closely spaced resonances and anti-resonances.

However, the difference in cumulative frequency values may not be all that large. The mean absolute difference in dB between the contaminated and exact RMS levels for the three 1/3 octaves was found to be 1.92, 0.11, and 4.27 dB, respectively. Such relatively moderate differences could ultimately justify the use of the patch technique by careful measurements, providing the results are band-averaged. However, it is too early to take a definite position about this point; further investigation is needed to clarify it.

The simplest way of carrying out practical measurements would be to replace the patch-averaged quantities by point quantities taken at the patch centres. One should bear in mind here that the results are obtained by a matrix inversion, Eq. (3), which is very sensitive to even small imperfections, as demonstrated by Fig. (12). Replacing the averaged results by centre values would introduce such type of imperfections. Patch coupling certainly uses a reduced number of data due to spatial averaging, but nevertheless all interface points participate in it. Coupling done by discrete points takes nothing else but the coupling points into account.

Fig. 13 shows the RMS sound pressure at the reception point obtained by point coupling in the case of interior excitation specified in §5.4. Contrary to previously shown cases using patch coupling, the results obtained by point coupling differ a lot from the exact ones. In this case even the 1/3-octave RMS levels of the exact and point-coupled values differ a lot: 3.69, −16.75, and −9.41 dB, respectively. It should be remembered that Fig. 13 applies to the theoretical case, free from signal contamination. The latter would certainly lead to a much larger mismatch with the exact values.

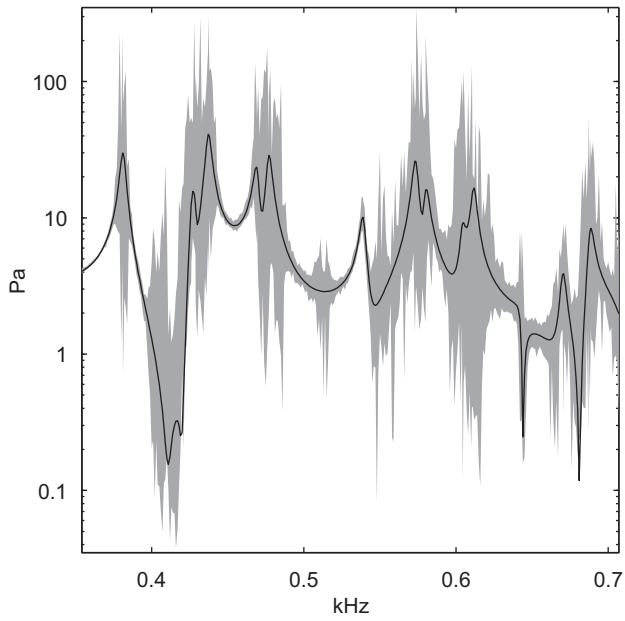

Fig. 12. Excitation by 2 pistons: reception point RMS sound pressure by patch coupling. ■: input data contaminated with random noise of 50 dB S/N ratio. ————: exact result.

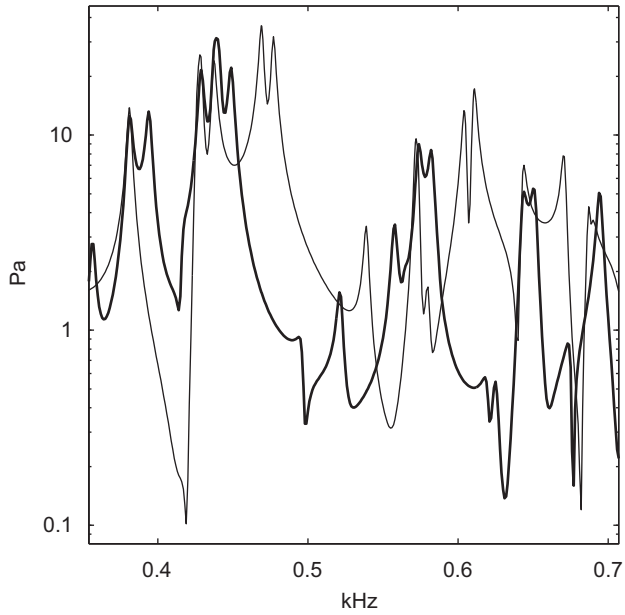

Fig. 13. Excitation by interior point sources: reception point RMS sound pressure. ————: solution by discrete point coupling; —: exact solution.

4. Conclusion

It has been shown that the characterization of a source and a receiver of air-borne sound using the patch impedance concept is potentially promising solution even if only a limited number of interface patches are employed. This fact may be of major importance for carrying out a particular type of sub-structuring suitable for virtual noise synthesis. The size of patches to be used depends on frequency: in the examples analysed the patch size of about 0.2 of the wavelength was found to give good results.

The patch approach requires matrix manipulations, out of which the inversion is sensitive to poor conditioning. The conditioning will become a problem if the patch input data, the source and receiver descriptors, are imperfect. This will normally be the case when such data are obtained by measurements. The contamination of measured data by noise could

severely degrade the conditioning and thus the quality of final results. In such cases the narrowband results are not likely to be directly exploitable. It is possible that band averaging may reduce the poor quality of results caused by measurement noise. However, the patch-averaging readings for obtaining the source and receiver descriptors from measurement should not be replaced by point readings as this may damage the results considerably.

It is hoped that the proposed approach can serve as a tool for noise synthesis of complex noise sources. The purpose of the present investigation was to check the validity of the patch coupling concept. Further investigations will be needed in order to fully assess the scope and the limitations of the present approach.

Appendix A. The demonstrator system

The complex amplitudes of sound pressure and volume velocity at any position x within the tube are given by well-known expressions ([26], Chapter II):

$$P(x) = P_+ e^{-jkx} + P_- e^{jkx}, \quad Q(x) = \frac{S}{\rho_0 c}(P_+ e^{-jkx} - P_- e^{jkx}) \tag{A1}$$

where P_+ and P_- are the complex pressure amplitudes of sound waves travelling in $+x$ and $-x$ directions, respectively, S is the tube cross section area, ρ_0 and c are the fluid mean mass density and sound speed, respectively and k is the wavenumber, $k=\omega/c$.

Using the boundary conditions $Q(0)=Q_0$ for the volume velocity of the piston at the driven end $x=0$ and $P(l)/Q(l)=Z_e$ at the opposite end $x=l$, the sound pressure amplitude at any point x can be obtained from (A1) as

$$P(x) = Q_0 \frac{\rho_0 c}{S} \frac{z_e \cos[k(l-x)] + j \sin[k(l-x)]}{\cos(kl) + j z_e \sin(kl)} \tag{A2}$$

where z_e denotes the non-dimensional impedance of the tube end, $z_e=Z_e S/\rho_0 c$.

The tube will be now split into two parts: the source and the receiver, Fig. 2. The two parts are delimited by a fictitious surface S, located at $x=a$. For the sake of simplicity this surface is chosen to be perpendicular to the tube axis. Having selected the interface surface S, the source now becomes the piston coupled to the volume of the tube between the piston and S. The receiver is the remaining part of the tube. As the sound pressure is uniformly distributed across S, a single patch suffices to achieve correct coupling. The matrix equations (3) and (4) become in this case ordinary algebraic equations.

The source needs to be characterised by two descriptors: its blocked pressure and its impedance. The blocked pressure is the pressure at S, with S made immobile. It can be thus obtained from (A1) by setting $Q(a)=0$. The other boundary condition required to solve (A1) is $Q(0)=Q_0$. This yields the amplitude of the blocked pressure:

$$P_b = Q_0 \frac{\rho_0 c}{jS \sin(ka)} \tag{A3}$$

The impedance of the source Z_s, seen from the coupling position $x=a$, will be obtained by switching the piston off, $Q_0=Q(0)=0$, and finding the pressure at $x=a$ due to unit velocity at the same point: $Z_s=P(a)/Q(a)$. Taking the sign as positive when the velocity is directed into the source, this gives

$$Z_s = \frac{\rho_0 c}{jS} \cot(ka) \tag{A4}$$

Finally, the receiver has to be characterised by its coupling impedance Z_r. To this end Eq. (A1) can be directly used by replacing Q_0 by unity, l by $l-a$ and x by 0:

$$Z_r = \frac{\rho_0 c}{S} \frac{z_e \cos[k(l-a)] + j \sin[k(l-a)]}{\cos[k(l-a)] + j z_e \sin[k(l-a)]} \tag{A5}$$

By applying Eq. (3) the coupling pressure between the source and the receiver can be found using expressions (A3)–(A5):

$$P_c = P(a) = \frac{Z_r}{Z_s + Z_r} P_b = Q_0 \frac{\rho_0 c}{S} \frac{z_e \cos[k(l-a)] + j \sin[k(l-a)]}{\cos(kl) + j z_e \sin(kl)} \tag{A6}$$

On the other hand, the last result can be obtained directly from (6) by selecting $x=a$. Thus the direct solution and the one obtained by patch sub-structuring give identical results. The results are strictly identical because the pressure distribution across the patch is uniform in the present case, and thus the patch concept is not approximate any more.

Appendix B. 3D patch coupling of parallelepipedic spaces

In this section formulae will be derived for patch sub-structuring applied to parallelepipedic spaces. Both the source and the receiver will be modelled as parallelepipedic acoustical volumes. Such a geometry enables the use of an analytical solution which is needed in the analysis to follow.

Within a cavity of substantially rigid walls the pressure response amplitude P at a point $\mathbf{r}$ due to a point source excitation of volume velocity amplitude Q at a point $\mathbf{r}_e$ can be obtained by conventional modal summation:

$$P(\mathbf{r}) = \mathrm{j}Q(\mathbf{r}_e)\frac{\rho_0 c^2}{V}\sum_n \frac{\phi_n(\mathbf{r})\phi_n(\mathbf{r}_e)}{\omega_n^2-\omega^2+2\mathrm{j}\varepsilon\omega} = Q(\mathbf{r}_e)\sum_n \boldsymbol{\Phi}_n(\mathbf{r},\mathbf{r}_e,\omega) \tag{B1}$$

where ω_n are the natural frequencies, ϕ are the normalised natural modes, ε is an equivalent damping coefficient, and V is the volume of the cavity. The symbol Φ is thus used for the modal contribution to sound pressure of the nth mode under unit excitation.

If the mean absorption coefficient of the cavity is α, $\alpha \ll 1$, the damping coefficient can be estimated by ([28], Chapter 6)

$$\varepsilon \approx \alpha\frac{cS}{2V} \tag{B2}$$

where S is the bounding surface of the cavity.

Let the acoustical volume considered be a parallelepiped of dimensions $a \times b \times h$, aligned with a x–y–z Cartesian system with one of the vertices at the origin. In such a case the natural frequencies satisfy the well-known relationship:

$$\omega_n = \frac{\pi}{c}\sqrt{\left(\frac{m_x(n)}{a}\right)^2+\left(\frac{m_y(n)}{b}\right)^2+\left(\frac{m_z(n)}{h}\right)^2}, \quad m_x,m_y,m_z = 0,1,2\ldots \tag{B3}$$

with the integers $m(n)$ chosen to give a monotonous increase of ω_n with n increasing, $n=1, 2\ldots$. The normalised natural modes can be put in a factorised form:

$$\phi_n(x,y,z) = \zeta(n)\cos\left(\frac{m_x(n)\pi x}{a}\right)\cos\left(\frac{m_y(n)\pi y}{b}\right)\cos\left(\frac{m_z(n)\pi z}{h}\right)$$
$$\zeta(n) = \sqrt{2^s}, s = \mathrm{sgn}(m_x)+\mathrm{sgn}(m_y)+\mathrm{sgn}(m_z) \tag{B4}$$

Within a given cavity the patches used for coupling have to be placed at the cavity boundary surfaces. In the case of a parallelepiped the position of coupling patches will thus be at one or several sides. Take now a rectangular patch perpendicular to the x-axis with the lateral and vertical sides Δy and Δz, centred at a point $[x_0, y_0, z_0]$. The mean value of sound pressure across this patch of surface $\Delta S=\Delta y\Delta z$, excited by a point source of strength Q at $\mathbf{r}_e$, can be found by integrating Eq. (B1):

$$\langle P(x_0,y_0,z_0)\rangle_{\Delta S} = \frac{1}{\Delta S}\int_{\Delta S} p(\mathbf{r})\,dS = \mathrm{j}Q\frac{\rho_0 c^2}{V}\sum_n \frac{\phi_n(\mathbf{r}_e)}{\omega_n^2-\omega^2+2\mathrm{j}\varepsilon\omega}\frac{1}{\Delta S}\int_{\Delta S}\varphi_n(\mathbf{r})\,dS \tag{B5}$$

In the case of a parallelepiped the integral on the right can be found analytically:

$$\frac{1}{\Delta S}\int_{\Delta S}\phi_n(r)\,dS = \zeta(n)\cos\left(\frac{m_x\pi x_0}{a}\right)\frac{1}{\Delta x\,\Delta y}\int_{y_0-\frac{\Delta y}{2}}^{y_0+(\Delta y/2)}\int_{z_0-\frac{\Delta z}{2}}^{z_0-(\Delta z/2)}\cos\left(\frac{m_y\pi y}{b}\right)\cos\left(\frac{m_z\pi z}{h}\right)dy\,dz$$
$$= \zeta(n)\cos\left(\frac{m_x\pi x_0}{a}\right)\cos\left(\frac{m_y\pi y_0}{b}\right)\mathrm{sinc}\left(\frac{m_y\,\Delta y}{2b}\right)\cos\left(\frac{m_z\pi z_0}{h}\right)\mathrm{sinc}\left(\frac{m_z\,\Delta z}{2h}\right)$$
$$= \phi_n(x_0,y_0,z_0)\gamma_{x,n}(m_y,m_z), \gamma_{x,n} = \mathrm{sinc}\left(\frac{m_y(n)\,\Delta y}{2b}\right)\mathrm{sinc}\left(\frac{m_z(n)\,\Delta z}{2h}\right) \tag{B6}$$

with sinc denoting the cardinal sine, $\mathrm{sinc}(u)=\sin(\pi u)/(\pi u)$. It can be thus seen that the averaging of sound pressure across a patch centred at $\mathbf{r}_0$ is equivalent to weighting the modes at $\mathbf{r}_0$ by a function γ_x specific of the patch size. Since $|\mathrm{sinc}(u)| \le 1$, the averaging will represent some sort of weakening of the modal contributions, the more the larger the patch size.

The index x of the function γ_x signifies that the averaging is done in the y–z plane, perpendicular to x. The averaging across the patches $\Delta x \times \Delta z$ and $\Delta x \times \Delta y$ in the x–y and x–z planes gives

$$\gamma_{y,n} = \mathrm{sinc}\left(\frac{m_x(n)\,\Delta x}{2a}\right)\mathrm{sinc}\left(\frac{m_z(n)\,\Delta z}{2h}\right), \quad \gamma_{z,n} = \mathrm{sinc}\left(\frac{m_x(n)\,\Delta x}{2a}\right)\mathrm{sin}c\left(\frac{m_y(n)\,\Delta y}{2b}\right) \tag{B7}$$

The $\mathrm{sinc}(u)$ function displays lobes alternating from positive to negative values. The first zero-crossing is at 1. Theoretically, the coupling by patches should tend to the exact result with reducing the patch size toward zero. In this case the sinc function approaches unity. If the arguments of γ functions in Eqs. (B6) and (B7) are limited to values less than unity, the contribution of respective modes to the average patch pressure will be always constructive. Moreover, if an argument is inferior to 0.5, the associated mode contribution will be relatively high, between 60% and 100% of the exact amount. Ideally all the modes should contribute with a unit weighting (zero patch size) which allows formulating an ad-hoc criterion for the selection of patch size: the arguments of γ should not exceed 0.5 for the modes which are strongly excited.

The argument of the sinc function is of the type $m\Delta/2d$ where m is the number of modal half-wavelengths in the given direction and d is the cavity size in this direction. Thus the requirement $\arg(\gamma) < 0.5$ means that the patch size should not exceed half the modal wavelength in a given direction (here the modal wavelength is not to be confused with the wavelength of sound).

So far the patch averaging has been dedicated to the response, i.e. to sound pressure. This enables the modelling of the blocked pressure. In order to further apply the patch concept to the impedance, either that of the source or of the receiver, spatial averaging of the excitation has to be carried out as well.

The sound pressure at a point **r** due to an excitation of total strength Q, uniformly spread over a patch of the size ΔS, will read:

$$P(x,y,z) = \mathrm{j}Q\frac{\rho_0 c^2}{V}\sum_n \frac{\phi_n(\mathbf{r})}{\omega_n^2-\omega^2+2\mathrm{j}\varepsilon\omega}\frac{1}{\Delta S}\int_{\Delta S}\phi_n(\mathbf{r}_e)\,dS \tag{B8}$$

It is easy to show that the averaging across an excitation patch results in the same weighting functions as the ones obtained for the response patch averaging, i.e. $\gamma_{x,n}$, $\gamma_{y,n}$, and $\gamma_{z,n}$.

References

[1] T. Ten Wolde, G. Gadefelt, Development of standard measurement methods for structure-borne sound emission, *Noise Control Engineering Journal* 28 (1987) 5–14.
[2] J.M. Mondot, B.A.T. Petersson, Characterization of structure-borne sound sources: the source descriptor and the coupling function, *Journal of Sound and Vibration* 114 (1987) 507–518.
[3] B.A.T. Petersson, B.M. Gibbs, Use of the source descriptor concept in studies of multi-point and multi-directional vibrational sources, *Journal of Sound and Vibration* 168 (1993) 157–176.
[4] S. Jianxin, A.T. Moorhouse, B.M. Gibbs, Towards a practical characterization for structureborne sound sources based on mobility techniques, *Journal of Sound and Vibration* 185 (1995) 737–741.
[5] M.H.A. Janssens, J.W. Verheij, A pseudo-forces methodology to be used in characterization of structure-borne sound sources, *Applied Acoustics* 61 (2000) 285–308.
[6] B.A.T. Petersson, B.M. Gibbs, Towards a structure-borne sound source characterization, *Applied Acoustics* 61 (2000) 325–343.
[7] A.T. Moorhouse, A.S. Elliott, T.A. Evans, In situ measurement of the blocked force of structure-borne sound sources, *Journal of Sound and Vibration* 325 (2009) 679–685.
[8] M.L. Kathuriya, M.L. Munjal, Experimental evaluation of the aeroacoustic characteristics of a source of pulsating gas flow, *Journal of the Acoustical Society of America* 65 (1979) 240–248.
[9] M.G. Prasad, A four load method for evaluation of acoustical source impedance in a duct, *Journal of Sound and Vibration* 114 (1987) 347–356.
[10] H. Bodén, The multiple load method for measuring the source characteristics of time-variant sources, *Journal of Sound and Vibration* 148 (1991) 437–453.
[11] H. Bodén, M. Åbom, Modelling of fluid machines as sources of sound in duct and pipe systems, *Acta Acoustica* 3 (1995) 549–560.
[12] J. Lavrentjev, M. Åbom, H. Bodén, A measurement method for determining the source data of acoustic two-port sources, *Journal of Sound and Vibration* 183 (1995) 517–531.
[13] J. Lavrentjev, M. Åbom, Characterization of fluid machines as acoustic multi-port sources, *Journal of Sound and Vibration* 197 (1996) 1–16.
[14] S.-H. Jang, J.-G. Ih, Refined multiload method for measuring acoustical source characteristics of an intake or exhaust system, *Journal of the Acoustical Society of America* 107 (2000) 3217–3225.
[15] L. Cremer, Synthesis of the sound field of an arbitrary rigid radiator in air with arbitrary particle velocity distribution by means of spherical sound fields, *Acustica* 55 (1984) 44–47 in German.
[16] G. Koopmann, L. Song, J.B. Fahnline, A method for computing acoustic fields based on the principle of wave superposition, *Journal of the Acoustical Society of America* 88 (1989) 2433–2438.
[17] M. Ochmann, Multiple radiator synthesis—an effective method for calculating the radiated sound field of vibrating structures of arbitrary source configuration, *Acustica* 72 (1990) 233–246 in German.
[18] Yu.I. Bobrovnitskii, T.M. Tomilina, Calculation of radiation from finite elastic bodies by method of equivalent sources, *Soviet Physics Acoustics* 36 (1990) 334–338.
[19] G. Pavić, An engineering technique for the computation of sound radiation by vibrating bodies using substitute sources, *Acustica united with Acta Acustica* 91 (2005) 1–16.
[20] A.T. Moorhouse, G. Seiffert, Characterization of an airborne sound source for use in a virtual acoustic prototype, *Journal of Sound and Vibration* 296 (2006) 334–352.
[21] Yu.I. Bobrovnitskii, A theorem on representation of the field of forced vibrations of a composite elastic system, *Acoustical Physics* 47 (2001) 409–411.
[22] Yu.I. Bobrovnitskii, G. Pavić, Modelling and characterization of airborne noise sources, *Journal of Sound and Vibration* 261 (2003) 527–555.
[23] J. O'Hara, Mechanical impedance and mobility concepts, *Journal of the Acoustical Society of America* 41 (1967) 1180–1184.
[24] G. Pavić and N. Totaro, Noise source characterization using patch impedance technique. Archives (1992–2008) of the EUROpean Conference on NOISE Control, Paris, June–July 2008, CD-ROM, 2008, pp. 453–458.
[25] M. Ouisse, L. Maxit, C. Cacciolati, J.-L. Guyader, Patch transfer functions as a tool to couple linear acoustics problems, *Journal of Vibration and Acoustics* 127 (2005) 458–466.
[26] S.N. Rschevkin, in: *The Theory of Sound*, Pergamon student editions, Oxford, 1963.
[27] Lord Rayleigh, in: *The Theory of Sound, Vol. II*, 2nd edition, Dover, New York, 1945.
[28] A.D. Pierce, in: *Acoustics*, McGraw Hill, New York, 1981.
[29] M. Aucejo, L. Maxit, N. Totaro and J.-L. Guyader, Introduction of residual modes concept in the patch transfer functions method to model the structure–acoustic coupling in heavy fluid. P*roceedings of the 16th International Congress on Sound and Vibration*, Krakow, July 2009, CD-ROM paper 711.
[30] L. Gavrić, G. Pavić, A finite element method for computation of structural intensity by the normal mode approach, *Journal of Sound and Vibration* 164 (1993) 29–43.